

# Tree-cotree gauging for two-dimensional hierarchical splines

M. Merkel<sup>[0000-0002-2104-9167]</sup> and R. Vázquez

**Abstract** In magnetostatics and eddy current problems, formulated in terms of the magnetic vector potential, the solution is not unique, because the addition of an irrotational function to the solution remains a valid solution. The tree-cotree decomposition is a gauging technique to recover uniqueness when using finite elements, and it consists in considering the mesh as a graph, and building a spanning tree on that graph. The idea has been recently extended to isogeometric analysis, applying the construction of the spanning tree on the control mesh, or equivalently, on the Greville grid. In the present paper we extend the construction to hierarchical splines, a set of splines with multi-level structure for adaptive refinement, by constructing a spanning tree for each single level. Since for degree  $p = 1$  the spaces of finite elements and hierarchical splines coincide, the presented construction is also valid for quadrilateral finite element meshes with hanging nodes. To assess the correctness of the method, we present numerical results for the Maxwell eigenvalue problem.

## 1 Introduction

The equations for magnetostatics and magneto-quasistatics, or eddy currents, which describe the solution of slowly varying magnetic fields [12], are commonly formulated in terms of the magnetic vector potential. For example, assuming homogeneous boundary conditions, the magnetostatic formulation is given by

---

M. Merkel

Computational Electromagnetics Group and Centre for Computational Engineering, Technische Universität Darmstadt, Darmstadt, Germany e-mail: melina.merkel@tu-darmstadt.de

R. Vázquez

Departamento de Matemática Aplicada, Universidade de Santiago de Compostela, Santiago de Compostela, Spain and Galician Centre for Mathematical Research and Technology (CITMAga), Santiago de Compostela, Spain e-mail: rafael.vazquez@usc.es

$$\int_{\Omega} \nu \mathbf{curl} \mathbf{A}_h \cdot \mathbf{curl} \mathbf{v}_h \, d\Omega = \int_{\Omega} \mathbf{J}_{\text{src}} \cdot \mathbf{v}_h \, d\Omega, \quad \text{for all } \mathbf{v}_h \in V_h, \quad (1)$$

where  $\nu$  is the magnetic reluctivity,  $\mathbf{J}_{\text{src}}$  is an excitation current and  $V_h \subset \mathbf{H}_0(\mathbf{curl}; \Omega)$  is a curl-conforming discrete space. These formulations are usually discretized with edge finite elements, and it is known that the solution is unique up to an irrotational field. To recover uniqueness, one of the possible gauging techniques, which works directly at discrete level, is tree-cotree gauging [1, 18, 19]. The idea of the method is to consider the vertices and edges of the finite element mesh as nodes and edges of a graph, and then construct a spanning tree on this graph. The spanning tree is a subgraph that passes through every node without closing any loop, and it contains as many edges as the number of nodes minus one. Selecting the basis functions associated to edges in the complementary of the tree, which is called the cotree, leads to a linear system which is uniquely solvable. The application of tree-cotree techniques to high order finite elements can be achieved either with hierarchical conforming elements<sup>1</sup> [22], applying the tree construction only to low order functions, or with a careful construction of the basis of edge elements [2].

An alternative to high order finite elements that has gained popularity is isogeometric analysis (IGA), a discretization method based on splines [11], and an analogue to edge finite elements are the curl-conforming spline spaces introduced in [5]. It has been shown in [13] that tree-cotree techniques can be easily generalized in the case of tensor-product splines, by exploiting the existence of commutative isomorphisms between spline spaces and finite element spaces defined in an auxiliary grid, called the Greville grid. Tree-cotree techniques in IGA have also been used to explicitly construct a basis of cohomology generators for formulations in terms of the scalar magnetic potential [14], and also in conjunction with domain decomposition methods [17].

One of the drawbacks of the spline spaces from [5] is their tensor-product structure, which only permits global refinement. To remove this constraint, spaces with local refinement capabilities have been studied in recent years in IGA, with (truncated) hierarchical B-splines being probably the most popular ones [24, 9]. They are based on a simple multi-level structure, where the space of each level is tensor-product, and the set of active functions from each level is chosen from their supports. As for the tensor-product case, curl-conforming spaces with hierarchical splines have been introduced in [8], along with certain conditions on the hierarchical meshes to guarantee the absence of spurious harmonic functions [8, 23].

While the construction of the tree to gauge the problem is easy for tensor-product splines, the extension to hierarchical splines is not obvious. It is not possible to build a global tree across all refinement levels, because the correspondence with finite elements in an auxiliary grid does not hold anymore. Moreover, the meshes of hierarchical splines are analogous to quadrilateral/hexahedral meshes with hanging nodes in finite elements, and we are not aware of any extension of tree-cotree gauging in this setting, although a multi-level gauging has been presented in [10]. In this paper we introduce tree-cotree techniques for spaces of hierarchical splines in simply connected domains with full Dirichlet boundary: exploiting the multi-level structure of hierarchical splines, a tree is

<sup>1</sup> The construction of hierarchical finite elements, where new functions are added for each degree, is different from hierarchical B-splines, where functions are added and removed at each level.

built for each level, creating an object that we define as a multi-level tree. We present the algorithm for the construction of the tree, and we show that it provides a valid gauge using numerical tests. It is also worth to remark that, for degree  $p = 1$ , hierarchical spline spaces coincide with finite elements. Therefore, our method provides an extension of tree-cotree gauging to finite element meshes with hanging nodes.

The outline of the paper is as follows. In Section 2 we recall the main concepts to define the tensor-product spline spaces on a single level, and the associated Greville grid in which we build the tree. Section 3 introduces the definitions of hierarchical splines, and extends the concept of Greville grids to Greville subgrids, which will be necessary to define the multi-level tree. The construction of the tree is detailed in Section 4, along with the algorithm to build it in practice. The correctness of the computed gauge is validated in Section 5 by numerical tests, solving the Maxwell eigenvalue problem to prove that gauging does not affect the computed eigenvalues.

## 2 Splines defined on a single level

In this section we introduce the spline de Rham sequence for dimension two, both for single-patch and multi-patch domains. These spaces will be used to construct the corresponding sequences of hierarchical splines in the next section. We also present the definition of the Greville grids, that will be necessary to apply the tree-cotree gauging in Section 4.

### 2.1 Spline de Rham sequence in a single-patch domain

Given two integers  $n > 0$  and  $p > 0$ , and a knot vector  $\Xi = \{\xi_1, \xi_2, \dots, \xi_{n+p+1}\}$ , with  $0 = \xi_1 \leq \xi_2 \leq \dots \leq \xi_{n+p+1} = 1$ , the B-spline basis of degree  $p$  is obtained using the Cox-de Boor formula, and we denote by  $S_p(\Xi)$  the corresponding spanned space. Multivariate B-splines of degree  $p$  are defined in the unit square  $\widehat{\Omega} = (0, 1)^2$  by tensor-product, from given values  $n_1, n_2 > 0$  and knot vectors  $\Xi_1, \Xi_2$ . It is well known that a discrete de Rham sequence can be constructed using B-splines of mixed degrees  $p$  and  $p - 1$  [5, 4]. We will denote the spaces of the sequence as  $\widehat{X}^k$ , for  $k = 0, 1, 2$ . For this work, we are mainly interested in the first two spaces, which are defined as

$$\begin{aligned}\widehat{X}^0 &= S_p(\Xi_1) \otimes S_p(\Xi_2), \\ \widehat{X}^1 &= S_{p-1}(\Xi'_1) \otimes S_p(\Xi_2) \times S_p(\Xi_1) \otimes S_{p-1}(\Xi'_2),\end{aligned}$$

where  $\Xi'_i$  is built from  $\Xi_i$  removing the first and last knots. Moreover, we also denote by  $\widehat{\mathcal{B}}^k$  the basis for  $\widehat{X}^k$ , for  $k = 0, 1, 2$ , which is built from standard B-splines for degree  $p$  and Curry-Schoenberg splines for degree  $p - 1$ , as in [21].

We assume that our physical domain  $\Omega \subset \mathbb{R}^2$  is a surface constructed through a parametrization  $\mathbf{F} : \widehat{\Omega} \rightarrow \Omega$  and, as standard in IGA, in practice it will be defined

by splines or NURBS, with the same degree and continuity as  $\widehat{X}^0$ . Then, the discrete spaces  $X^k$  in the physical domain are defined by suitable pull-backs, and in particular we have

$$X^0(\Omega) = \{u : u \circ \mathbf{F} \in \widehat{X}^0\}, \quad X^1(\Omega) = \{\mathbf{u} : D\mathbf{F}^\top(\mathbf{u} \circ \mathbf{F}) \in \widehat{X}^1\},$$

where  $D\mathbf{F}$  is the Jacobian of the parametrization. The bases  $\mathcal{B}^k$  are defined applying the same pull-backs to the basis functions in the parametric domain.

## 2.2 Spline de Rham sequence in multi-patch domains

More complex domains can be defined using multi-patch techniques. We assume that the domain is formed by several patches  $\overline{\Omega} = \bigcup_{i=1}^{N_p} \overline{\Omega}^{(i)}$ , each patch parametrized in the form  $\mathbf{F}^{(i)} : \widehat{\Omega} \rightarrow \Omega^{(i)}$  and satisfying that  $\Omega^{(i)} \cap \Omega^{(j)} = \emptyset$  for  $i \neq j$ . Moreover, we assume that  $\partial\Omega^{(i)} \cap \partial\Omega^{(j)}$  corresponds to either a vertex or a full edge for each patch. Assuming that the two parametrizations at the interfaces coincide up to an affine transformation, and that the same holds for their corresponding knot vectors, one can define discrete conforming spaces in the multi-patch domain as

$$\begin{aligned} X^0(\Omega) &= \{u \in H^1(\Omega) : u|_{\Omega^{(i)}} \in X^0(\Omega^{(i)})\}, \\ X^1(\Omega) &= \{\mathbf{u} \in \mathbf{H}(\mathbf{curl}; \Omega) : \mathbf{u}|_{\Omega^{(i)}} \in X^1(\Omega^{(i)})\}. \end{aligned}$$

In this situation, there is a one-to-one correspondence between functions of neighboring patches that do not vanish on the interface, and they can be identified up to orientation, as it is done in finite elements. We refer the reader to [6, Sect. 4.4] for the details on how to define the spaces in the multi-patch setting. By abuse of notation, we will denote in the same way the bases of the single-patch and multi-patch cases, namely  $\mathcal{B}^k$ .

## 2.3 The Greville grid and auxiliary finite element spaces

In the univariate setting, each basis function is associated to a Greville abscissa defined by the knot average  $P_i = (\xi_{i+1} + \dots + \xi_{i+p})/p$ , for  $i = 1, \dots, n$ . In the unit square, we can associate to each basis function in  $\widehat{\mathcal{B}}^0$  a Greville point, defined as the Cartesian product of univariate points, and map them through  $\mathbf{F}$  to obtain the corresponding Greville points for  $\mathcal{B}^0$ , the basis functions in the physical domain. By connecting the Greville points we obtain a Cartesian grid in the parametric domain  $\widehat{\Omega}$ , and a structured grid of bilinear quadrilaterals that approximate the physical domain  $\Omega$ . We will refer to this as the Greville grid, and it will be denoted by  $G$ . By construction, the basis functions in  $\mathcal{B}^0$  are associated to the nodes of the Greville grid, while the basis functions in  $\mathcal{B}^1$  are associated to its edges. Moreover, we can define in the grid  $G$  the discrete spaces of lowest order nodal elements and lowest order finite edge elements, that we

denote by  $Z^0$  and  $Z^1$ . Then, identifying each basis function of the spline spaces with the corresponding basis functions of these auxiliary finite element spaces, there exist linear isomorphisms  $I^0, I^1$  such that the following diagram commutes [6]

$$\begin{array}{ccc} X^0(\Omega) & \xrightarrow{\text{grad}} & X^1(\Omega) \\ I^0 \downarrow & & \downarrow I^1 \\ Z^0 & \xrightarrow{\text{grad}} & Z^1. \end{array} \quad (2)$$

In the multi-patch setting, due to the assumptions on how the patches are defined, the Greville points at the interface between two neighboring patches coincide. Therefore, it is possible to associate a Greville grid to the spline spaces also in this more general setting, with the difference that the grid is structured on each patch, but globally unstructured. The finite element spaces and the isomorphisms can also be defined in the multi-patch setting, and abusing notation, we will denote them as in the single-patch case. Examples of Greville grids are shown in Figure 1. To simplify the presentation, in the following the examples will be given for single-patch domains, and the visualization will be done for the Greville grid of the parametric domain.

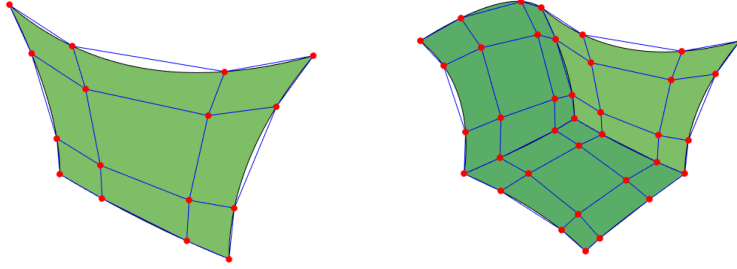


Fig. 1: Example of two-dimensional Greville grids for the single-patch (left) and multi-patch case (right).

*Remark 1* The Greville grid and the lowest order finite element spaces are auxiliary tools for the tree-cotree algorithm that will be introduced afterwards. Since the tree-cotree algorithm is based on topological properties, any other mesh with the same number of nodes and edges, and the same connectivity, would also work.

### 3 Hierarchical B-splines

Hierarchical splines are defined using a multi-level structure. First, we define standard spaces of splines on each level, as in the previous section, that can be either single-patch

or multi-patch. Then, by choosing the regions where we want to apply local refinement, we apply a selection algorithm in which basis functions are activated according to the relation of their supports with these regions [15, 24]. While the focus will be on the first two spaces of the de Rham sequence, for completeness we introduce the notation for the whole sequence, introduced in [8].

From now on we will assume that the spaces have vanishing boundary conditions, i.e., we will work with  $X^0(\Omega) \cap H_0^1(\Omega)$  and  $X^1(\Omega) \cap \mathbf{H}_0(\mathbf{curl}; \Omega)$ . To simplify notation, we will use the same notation  $X^0(\Omega)$  and  $X^1(\Omega)$  for the spaces with vanishing boundary conditions.

### 3.1 Definition of hierarchical splines

We start defining for  $k = 0, 1, 2$  a sequence of nested spline spaces

$$X_0^k \subset X_1^k \subset \dots \subset X_{L-1}^k \subset X_L^k,$$

where for every level  $\ell$ , the spaces  $X_\ell^k$  for  $k > 0$  are defined from  $X_\ell^0$ , and they form a de Rham sequence as in the previous section. We denote the basis for each of these spaces by  $\mathcal{B}_\ell^k$ , for each level  $\ell = 0, \dots, L$ . Moreover, we notice that at each level we have a Greville grid  $G_\ell$ .

To define hierarchical B-splines, we also need a nested sequence of closed subdomains

$$\overline{\Omega} = \Omega_0 \supseteq \Omega_1 \supseteq \dots \supseteq \Omega_L \supseteq \Omega_{L+1} = \emptyset,$$

where each subdomain is defined as the union of supports of functions from the previous level, namely

$$\Omega_{\ell+1} = \bigcup_{\beta \in \mathcal{S}_\ell} \overline{\text{supp } \beta}, \quad \text{for some } \mathcal{S}_\ell \subset \mathcal{B}_\ell^2, \ell = 0, \dots, L-1. \quad (3)$$

Let us define, for  $\ell = 0, \dots, L$  and  $\ell' \in \{\ell, \ell+1\}$ , the subset of basis functions with (open) support completely contained in  $\Omega_{\ell'}$ , namely

$$\mathcal{B}_{\ell, \ell'}^k = \{\beta \in \mathcal{B}_\ell^k : \text{supp } \beta \subset \Omega_{\ell'}\}.$$

Then, the basis of hierarchical B-splines  $\mathcal{H}_L^k$  is defined, for  $k = 0, 1, 2$ , by applying the following recursive algorithm:

1.  $\mathcal{H}_0^k = \mathcal{B}_0^k$ ,
2.  $\mathcal{H}_{\ell+1}^k = (\mathcal{H}_\ell^k \setminus \mathcal{B}_{\ell, \ell+1}^k) \cup \mathcal{B}_{\ell+1, \ell+1}^k$ , for  $\ell = 0, \dots, L-1$ .

That is, we start from the basis of tensor-product B-splines for the coarsest space, and at each step we remove coarse basis functions with support contained in  $\Omega_{\ell+1}$ , and add fine basis functions with support contained in the same subdomain. It has been proved in [24] (see also [8]) that the functions in  $\mathcal{H}_\ell^k$  are linearly independent for any  $\ell$ . We will denote by  $W_\ell^k = \text{span}\{\mathcal{H}_\ell^k\}$  the space of hierarchical B-splines up to level  $\ell$ .

We also define the set of active basis functions of level  $\ell$ , and the set of deactivated functions of level  $\ell$ , respectively as

$$\mathcal{A}_\ell^k = (\mathcal{B}_{\ell,\ell}^k \setminus \mathcal{B}_{\ell,\ell+1}^k), \quad \mathcal{D}_\ell^k = \mathcal{B}_{\ell,\ell+1}^k. \quad (4)$$

It is easy to see, due to the nestedness of the subdomains, that  $\mathcal{H}_\ell^k = (\bigcup_{\ell'=0}^{\ell-1} \mathcal{A}_{\ell'}^k) \cup \mathcal{B}_{\ell,\ell}^k = (\bigcup_{\ell'=0}^{\ell} \mathcal{A}_{\ell'}^k) \cup \mathcal{D}_\ell^k$ , and as a consequence  $\mathcal{H}_L^k = \bigcup_{\ell=0}^L \mathcal{A}_\ell^k$ , because  $\Omega_{L+1} = \emptyset$ .

### 3.2 The Greville subgrids and associated finite element spaces

We now introduce the Greville subgrids, that will play a prominent role in the tree-cotree decomposition. Following [8], we denote by  $G_{\ell,\ell'}$ , with  $\ell' \in \{\ell, \ell+1\}$ , the Greville subgrid formed by the cells associated to basis functions in  $\mathcal{B}_{\ell,\ell'}^2$ , that is, functions of level  $\ell$  with support completely contained in  $\Omega_{\ell'}$ . We note that, by the definition of the basis and due to the support of B-splines, a basis function belongs to  $\mathcal{B}_{\ell,\ell'}$  if and only if it is associated to an internal entity of the subgrid  $G_{\ell,\ell'}$ . Accordingly, basis functions associated to boundary entities do not belong to  $\mathcal{B}_{\ell,\ell'}$ . This motivates the presentation for vanishing boundary conditions, to treat in the same manner all the boundary entities of the Greville subgrid. By abuse of notation, we will also denote by  $G_{\ell,\ell'}$  the domain covered by the union of the cells in the Greville subgrid.

In Figure 2 we present two examples of Greville subgrids for hierarchical splines of degrees  $p = 1$  and  $p = 2$ . First of all, note that for degree  $p = 1$  there is a clear correspondence between the hierarchical mesh and the Greville subgrids, but this is lost when increasing the degree, due to the definition of the Greville points as knot averages. In fact, due to the difference of the knot averages between levels, the domains  $G_{\ell,\ell+1}$  and  $G_{\ell+1,\ell+1}$  are in general not equal, even if both correspond to functions with support contained in  $\Omega_{\ell+1}$ . These geometric differences between the grids will not be important for the tree-cotree decomposition, because the construction of the tree will be based on the topology of the mesh. We also remark that the active entities associated to active functions in  $\mathcal{A}_\ell^k$  of the hierarchical basis are contained in the closure of the subdomain  $G_{\ell,\ell} \setminus G_{\ell,\ell+1}$ , while those associated to deactivated functions are contained in the interior of  $G_{\ell,\ell+1}$ .

### 3.3 Constraints for exactness of the sequence

Although the construction of the de Rham sequence of hierarchical splines is possible for any hierarchical mesh, there are situations in which the spaces of hierarchical splines  $W^k(\Omega)$  do not form an exact sequence, and this may cause the appearance of spurious results. A necessary and sufficient condition for exactness was first identified in [8, Thm. 5.5]. However, in the same paper it was shown that there exist situations in which the sequence is exact, but spurious results still appear. For this reason the authors

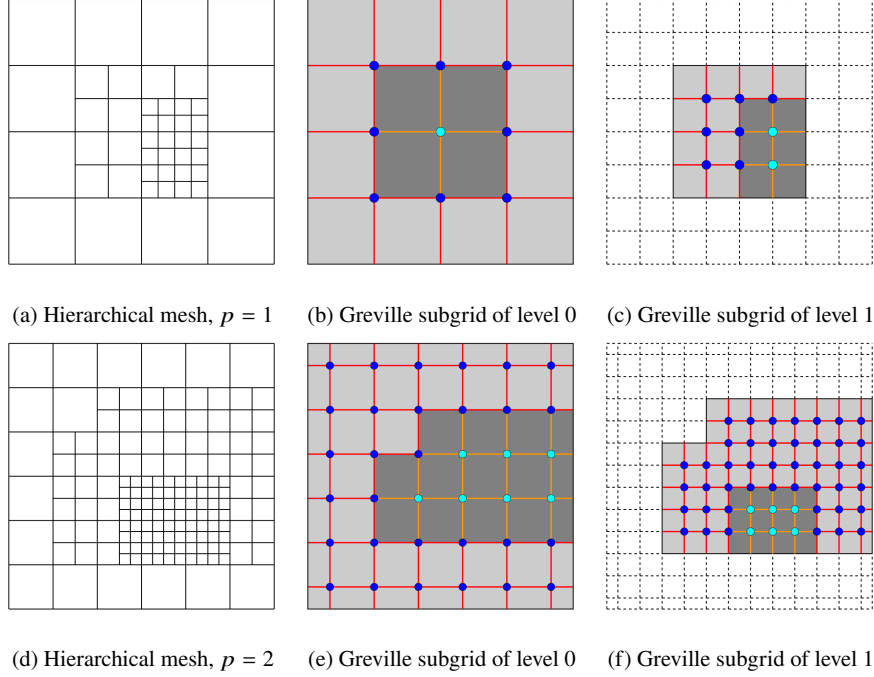


Fig. 2: Example for degrees  $p = 1$  (top row) and  $p = 2$  (bottom row) of hierarchical meshes with three levels (left), and the corresponding Greville subgrids for levels  $\ell = 0$  (center) and  $\ell = 1$  (right). The Greville subgrid  $G_{\ell,\ell}$  corresponds to all the highlighted gray region, and the Greville subgrid  $G_{\ell,\ell+1}$  corresponds to the dark gray region. The entities of the Greville subgrids associated to active basis functions are marked with blue vertices ( $\mathcal{A}_\ell^0$ ) and red edges ( $\mathcal{A}_\ell^1$ ), while those associated to deactivated functions are marked with cyan vertices ( $\mathcal{D}_\ell^0$ ) and orange edges ( $\mathcal{D}_\ell^1$ ). Note that all the internal entities of  $G_{\ell,\ell+1}$  correspond to deactivated functions.

introduced a sufficient condition for exactness based on the structure of the hierarchical mesh, which reads as follows

**Assumption 1.** For each level  $\ell = 0, \dots, L$  and for any basis function  $\beta \in \mathcal{B}_\ell^k$ , with  $k = 0, 1, 2$ , the region  $\text{supp } \beta \cap (\Omega \setminus \overline{\Omega_{\ell+1}})$  is connected and simply connected.

Another sufficient condition, which covers different cases, was presented in [23], with the main advantage that it can be generalized to arbitrary dimension. We also remark that a refinement algorithm that automatically satisfies this condition was recently introduced, in the two-dimensional case, in [7].

**Assumption 2.** Let us assume that in (3) we have  $\mathcal{S}_\ell \subset \mathcal{B}_\ell^0$ . Moreover, let  $\beta_1, \beta_2 \in \mathcal{B}_{\ell,\ell+1}^0$ . If they share an  $(\ell + 1)$ -intersection, as in [23, Def. 4.1] with  $n = 2$ , they must be connected through a shortest chain of functions in  $\mathcal{B}_{\ell,\ell+1}^0$ , as in [23, Def. 4.3].



The condition consists of two parts: first, we assume that the refined region is the union of support of functions in  $\mathcal{B}_\ell^0$  instead of  $\mathcal{B}_\ell^2$ , that is, they have degree  $p$  instead of degree  $p - 1$ . Second, whenever two refined functions are too close, there must be other refined functions in between that connect them. We remark that the condition appearing in [23], to which we refer for the details, is a bit more complex, because it covers situations that do not occur in the two-dimensional case.

The analysis of these conditions is beyond the focus of this paper. Therefore, without further details, from now on we will assume that the hierarchical meshes satisfy either Assumption 1 or Assumption 2.

## 4 Tree-cotree decomposition for hierarchical B-splines

As already mentioned in the introduction, the solution of the magnetostatic problem (1) is not unique, and a similar issue arises in the formulation of the magneto-quasistatic problem. One of the techniques to recover uniqueness for lowest order finite elements is tree-cotree gauging. In this section we will start presenting the basics of the tree-cotree decomposition for finite elements, and its extension to splines of one single level, introduced for the first time in [13]. Then, we will present the extension to multilevel hierarchical splines, including the algorithm to construct what we call a multi-level tree.

### 4.1 Tree-cotree gauging for splines of a single level

In order to apply tree-cotree gauging for low order finite elements, as explained in [1, 3, 18, 19] the idea is to consider the finite element mesh as a graph  $\mathcal{G} = (\mathcal{N}, \mathcal{E})$ , where the nodes  $\mathcal{N}$  and edges  $\mathcal{E}$  of the graph correspond to the vertices and edges of the mesh. Then, using an algorithm from graph theory, one builds a spanning tree  $\mathcal{T}$  on the graph. A spanning tree is a subgraph that passes through every node and that does not contain any cycle, and therefore, for a connected graph, it contains as many edges as the number of nodes minus one. Tree-cotree gauging is then applied by removing from the linear system the basis functions associated to the edges of the tree, or in other words, by keeping only those associated to the complementary of the tree, which is called the cotree. It is important to remark that, in order to take into account Dirichlet boundary conditions, the tree must be grown starting from the boundary. This kind of behavior can be obtained by constructing a minimum spanning tree, for instance using Kruskal's algorithm [16], and applying a lower weight to those edges associated to functions on which we impose Dirichlet boundary conditions. This procedure is also equivalent to collapse each connected component of the Dirichlet boundary into a single node [20].

The application of tree-cotree gauging for splines of a single level follows the same idea [13]. As it was explained in Section 2.3, the basis functions of the curl-conforming space are associated to the edges of the Greville grid. It is then sufficient to consider the Greville grid as a graph, and build the spanning tree on the Greville grid, applying exactly the same algorithms as in finite elements. Thanks to the isomorphisms between

the spline spaces and the auxiliary finite element spaces of the Greville grid (2), this will provide a valid gauge for the splines, by simply removing from the linear system the indices corresponding to basis functions associated to edges of the tree. We note that the construction is valid both in the single-patch or in the multi-patch case.

## 4.2 Tree-cotree gauging for hierarchical splines

The construction of the tree for splines on a single level is very simple, due to the existence of commutative isomorphisms with the auxiliary finite element spaces in the Greville grid. On the contrary, the extension to hierarchical splines is not obvious. In fact, it is not known if such isomorphisms exist for hierarchical splines, and even if that was the case, the corresponding Greville mesh across all levels would contain hanging nodes, as in the meshes of Figure 2. The presence of hanging nodes, that have no functions attached to them, prevents an easy interpretation of the mesh as a graph on which one can build the spanning tree, and in fact we are not aware of any application of tree-cotree gauging on finite element meshes with hanging nodes. Therefore, a new tree construction for the correct gauging of hierarchically refined B-splines is necessary and will be outlined in the following.

It is clear from (4) that the basis functions appearing in the hierarchical construction are related to the Greville subgrids. Indeed, the functions in  $\mathcal{B}_{\ell,\ell}^k$  and  $\mathcal{B}_{\ell,\ell+1}^k$  respectively correspond to the interior entities of  $G_{\ell,\ell}$  and  $G_{\ell,\ell+1}$ . In order to obtain a valid gauge we will build a spanning tree on the Greville subgrid of each level,  $G_{\ell,\ell}$ , with some constraints to ensure that the space of gradient fields of functions in  $W_L^0$  is correctly removed from the solution space  $W_L^1$ .

We start considering for each level  $\ell$  the Greville subgrid  $G_{\ell,\ell}$ , and define the graph  $\mathcal{G}_\ell = (\mathcal{N}_\ell, \mathcal{E}_\ell)$ , consisting of nodes and edges  $\mathcal{N}_\ell$  and  $\mathcal{E}_\ell$ , respectively. Note that the graph depends on the choice of the refined region  $\Omega_\ell$ , and it is not necessarily connected. Both the set of nodes and edges can be divided into entities in the interior of  $G_{\ell,\ell}$  and on its boundary  $\partial G_{\ell,\ell}$ , namely

$$\mathcal{N}_\ell = \mathcal{N}_\ell^{\text{int}} \cup \mathcal{N}_\ell^\partial, \quad \mathcal{E}_\ell = \mathcal{E}_\ell^{\text{int}} \cup \mathcal{E}_\ell^\partial.$$

Due to the definition of active functions, and since we are assuming vanishing boundary conditions, the boundary entities always correspond to non-active functions. Regarding the interior entities, they can be further divided into those associated to active basis functions in  $\mathcal{A}_\ell^k$  and deactivated basis functions in  $\mathcal{D}_\ell^k$ , with  $k = 0$  for the nodes and  $k = 1$  for the edges, namely

$$\mathcal{N}_\ell^{\text{int}} = \mathcal{N}_\ell^{\mathcal{A}} \cup \mathcal{N}_\ell^{\mathcal{D}}, \quad \mathcal{E}_\ell^{\text{int}} = \mathcal{E}_\ell^{\mathcal{A}} \cup \mathcal{E}_\ell^{\mathcal{D}}.$$

To achieve a correct gauging condition we propose the following approach. On each level  $\ell$  we construct a tree  $\mathcal{T}_\ell$  using the following three steps:

1. Construct a spanning tree on the boundary subgraph  $\mathcal{G}_\ell^\partial = (\mathcal{N}_\ell^\partial, \mathcal{E}_\ell^\partial)$ .
2. Grow the tree to the interior of  $G_{\ell,\ell}$  using active edges from  $\mathcal{E}_\ell^{\mathcal{A}}$ .

3. Grow the tree to the remaining nodes using deactivated edges from  $\mathcal{E}_\ell^{\mathcal{D}}$ .

That is, we first build a spanning tree on the boundary of  $G_{\ell,\ell}$  (or more precisely, on each connected component of the boundary of  $G_{\ell,\ell}$ ) using the boundary edges of the Greville subgrid, independently of whether they are associated to the Dirichlet boundary or not. Then, we grow the tree on active edges, which is equivalent to work in the closure of  $G_{\ell,\ell} \setminus G_{\ell,\ell+1}$ . Finally, the tree is grown on the region of deactivated functions,  $G_{\ell,\ell+1}$ , only if there are nodes that have not been reached. An illustration of the procedure is shown in Figure 3 for a simple mesh and degree  $p = 1$ .

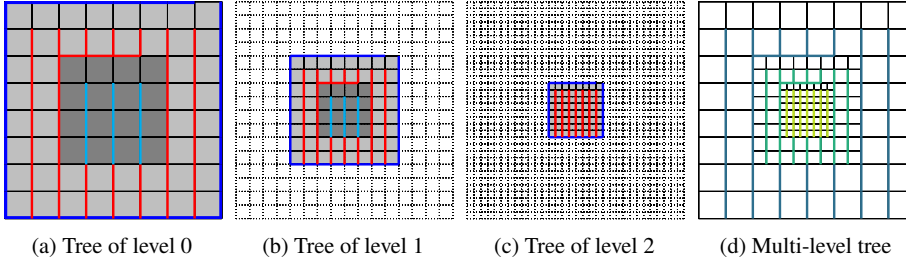


Fig. 3: Illustration of the trees built on each level for degree  $p = 1$ , for a three-level mesh. The first three figures show the tree of each single level, where the whole gray region corresponds to  $G_{\ell,\ell}$ , and the dark gray region corresponds to  $G_{\ell,\ell+1}$ . At each level, we first build the tree on the boundary of  $G_{\ell,\ell}$  (blue edges), then on the active edges (red edges), and finally on the deactivated edges (cyan edges). The right figure (d) shows the multi-level tree, combining active edges of the three levels.

With some abuse of notation, we will denote by  $\mathcal{T}_\ell^{\mathcal{A}}$  and  $\mathcal{T}_\ell^{\mathcal{D}}$  the restriction of the tree  $\mathcal{T}_\ell$  to edges associated to active and deactivated functions, respectively. The union of the active tree parts then defines the “multi-level tree”

$$\mathcal{M}_L = \bigcup_{\ell=0}^L \mathcal{T}_\ell^{\mathcal{A}}.$$

Since the multi-level tree consists of active edges, associated to active functions, we can define the multi-level cotree as the set of complementary active edges (or functions), and employ them for the decomposition of the linear system as in the single level case. We also show in Figure 3 a visualization of the multi-level tree. Note that the plot of the multi-level tree is not clear for degree greater than one, because, in the Greville submeshes, active edges of different levels would overlap.

In practice, the construction of the multi-level tree can be achieved working on each level independently. To build the tree on each level respecting the three steps, one can employ an algorithm to find a minimum spanning tree on weighted graphs, such as Kruskal’s algorithm [16]. The construction of the multi-level tree with such an algorithm is summarized in Algorithm 1.

**Algorithm 1** Construct multi-level tree  $\mathcal{M}_L$ 


---

```

 $\mathcal{M}_L \leftarrow \{\}$ 
for  $\ell = 0$  to  $L$  do
  Set weights of edges in  $\mathcal{E}_\ell^\partial$  to 1
  Set weights of edges in  $\mathcal{E}_\ell^{\mathcal{A}}$  to 2
  Set weights of edges in  $\mathcal{E}_\ell^{\mathcal{D}}$  to 3
  Find a minimum spanning tree  $\mathcal{T}_\ell$  on  $\mathcal{G}_\ell$  (e.g. using Kruskal's algorithm)
   $\mathcal{M}_L \leftarrow \mathcal{M}_L \cup \mathcal{T}_\ell^{\mathcal{A}}$ 
end for
return  $\mathcal{M}_L$ 

```

---

*Remark 2* The multi-level tree is not really a tree, because the union of Greville subgrids from different levels does not form a valid graph. We have decided to call this object a multi-level tree because it gives an idea of how it is constructed, and to maintain the *tree-cotree* nomenclature.

*Remark 3* We note that basis functions associated to deactivated edges  $\mathcal{E}_\ell^{\mathcal{D}}$  are not part of the hierarchical basis  $\mathcal{H}_L^1$ , and therefore they are not relevant for the final multi-level tree and cotree. In fact, in our configuration of a simply connected domain  $\Omega \subset \mathbb{R}^2$  with homogeneous boundary conditions, step 3 of the algorithm could be removed. However, the presence of deactivated functions is important if the domain has non-trivial topology. This will be the subject of a forthcoming paper for the three-dimensional case.

## 5 Numerical results

To numerically verify the correctness of the proposed tree-cotree decomposition for hierarchical B-splines, we solve the Maxwell eigenvalue problem in terms of the electric field strength  $\mathbf{E}$ . We write directly the discrete problem given in weak formulation by

$$\int_{\Omega} \nu \mathbf{curl} \mathbf{E}_h \cdot \mathbf{curl} \mathbf{E}'_h = \omega^2 \int_{\Omega} \epsilon \mathbf{E}_h \cdot \mathbf{E}'_h, \text{ for all } \mathbf{E}'_h \in V_h$$

where  $\mathbf{E}_h \in V_h$  and  $\omega \in \mathbb{R}$  are the unknown eigenmodes and eigenfrequencies, respectively, and the material properties  $\nu$  and  $\epsilon$  represent the magnetic reluctivity and the electric permittivity, for simplicity both are taken equal to one. The discrete space  $V_h \subset \mathbf{H}_0(\mathbf{curl}; \Omega)$  is chosen as the space of curl-conforming hierarchical splines,  $V_h = W_L^1$ .

For the solution of this problem with tree-cotree gauging, we follow the procedure explained in [18]. While the use of tree-cotree gauging is not particularly advantageous for the Maxwell eigenvalue problem, we chose it as a model problem because it serves to test the validity of the gauge. Indeed, when the eigenvalue problem is solved without a gauging method, one obtains zero eigenvalues associated to gradient fields, and their number corresponds to the dimension of the discrete kernel of the curl operator. If the problem is gauged correctly, these zero eigenvalues are removed from the solution

without affecting the remaining eigenvalues. If gauging is not applied correctly, spurious modes appear in the computed solution.

We present some numerical tests to test the validity of the tree-cotree decomposition. All the tests are performed using the GeopDEs library [25] in MATLAB 2025a, and the eigenvalue problem is solved using the `eig` command.

*Example 1 (Simple refinement in a square)* In the first numerical example the domain is the square  $\Omega = (0, \pi)^2$ , and we consider a simple refinement in the central part of the domain. Starting from an  $8 \times 8$  mesh, we refine at each step the central part consisting of a square of  $4 \times 4$  elements of the finest level, as in Figure 3. We stop the refinement at the third level. We solve the Maxwell eigenvalue problem with degrees  $p = 1$  and  $p = 3$ , and compare the eigenvalues computed applying tree-cotree gauging with the non-zero eigenvalues obtained with the ungauged formulation, which are considered to be correct.

The multi-level tree for degree  $p = 1$  is the one already displayed in Figure 3. The computed eigenvalues, that are shown in Figure 4, demonstrate that the construction of the multi-level tree provides a valid gauge. For degree  $p = 3$ , we plot separately the trees for the three levels in Figure 5. As already mentioned, a plot of the multi-level tree would not be clear, because the Greville subgrids of the different levels overlap. The comparison of the computed eigenvalues in Figure 6 confirms the validity of the gauge also for high degree.

*Example 2 (Refinement creating a hole)* In the second numerical test we consider again the square  $\Omega = (0, \pi)^2$ . Starting from an  $8 \times 8$  mesh, we now refine the elements in such a way that the refined region has a hole in it, see Figure 9d, and therefore the Greville subgrid of fine levels has non-trivial topology. We refine the mesh in such a way that it only has three levels. We plot in Figure 7 and Figure 9 the trees obtained for degrees  $p = 1$  and  $p = 3$ , respectively. We note that, although the Greville subgrids have holes in them, it is not necessary to apply any special treatment due to the topology, because all the boundaries are treated as Dirichlet boundary conditions. In fact, the spanning tree connects the two boundaries without issues. In Figure 8 and Figure 10 we plot the computed eigenvalues for the same degrees. As in the previous tests, there is no difference between the eigenvalues obtained for the problem without gauging or applying tree-cotree gauging. We can therefore conclude that the tree-cotree decomposition that we propose is correct also in this case.

## Acknowledgements

The work of Rafael Vázquez has been partially funded by Consellería de Educación, Ciencia, Universidades e Formación Profesional - Xunta de Galicia (2025-AD059 and ED431F 2025/03), and by the Spanish State Research Agency (PID2024-156071NB-I00). The work of Melina Merkel is supported by the joint DFG/WWF Collaborative Research Centre CREATOR (DFG: Project-ID 492661287/TRR 361; WWF: 10.55776/F90) at TU Darmstadt, TU Graz and JKU Linz, by the LOEWE Project

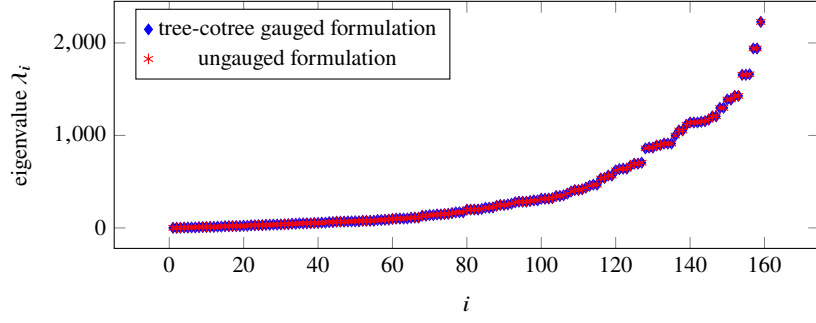


Fig. 4: Eigenvalues of the Maxwell eigenvalue problem of Example 1 for  $p = 1$  computed applying tree-cotree gauging and non-zero eigenvalues of the ungauged formulation.

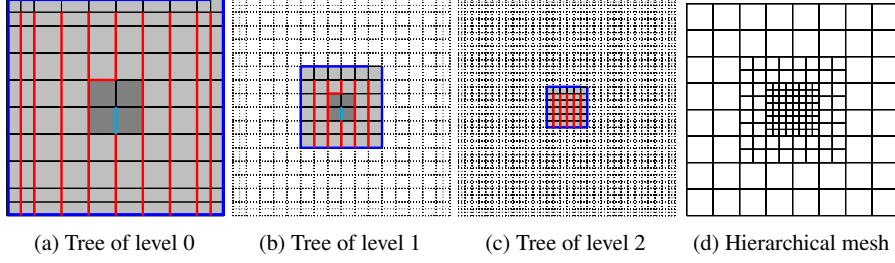


Fig. 5: Illustration of the trees built on each level for degree  $p = 3$ , for Example 1. The first three figures (a)-(c) show the tree of each single level, where the whole gray region corresponds to  $G_{\ell,\ell}$ , and the dark gray region corresponds to  $G_{\ell,\ell+1}$ . The blue edges correspond to the edges on the boundary of  $G_{\ell,\ell}$ , the red edges to the active edges, and the cyan edges to the deactivated edges. The right figure (d) shows the hierarchical mesh.

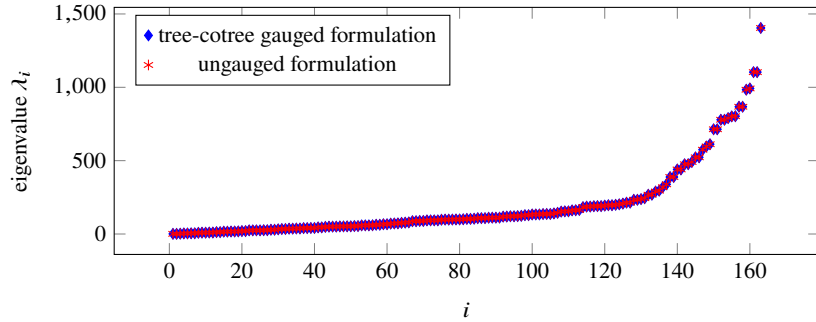


Fig. 6: Eigenvalues of the Maxwell eigenvalue problem of Example 1 for  $p = 3$  computed applying tree-cotree gauging and non-zero eigenvalues of the ungauged formulation.

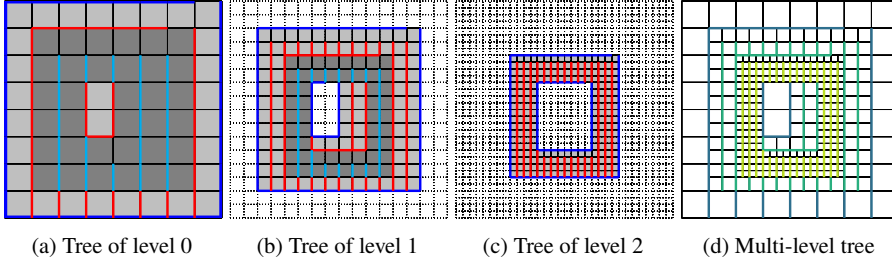


Fig. 7: Illustration of the trees built on each level for degree  $p = 1$ , for Example 2. The first three figures (a)-(c) show the tree of each single level, where the whole gray region corresponds to  $G_{\ell,\ell}$ , and the dark gray region corresponds to  $G_{\ell,\ell+1}$ . The blue edges correspond to the edges on the boundary of  $G_{\ell,\ell}$ , the red edges to the active edges, and the cyan edges to the deactivated edges. The right figure (d) shows the multi-level tree, combining edges of the three levels.

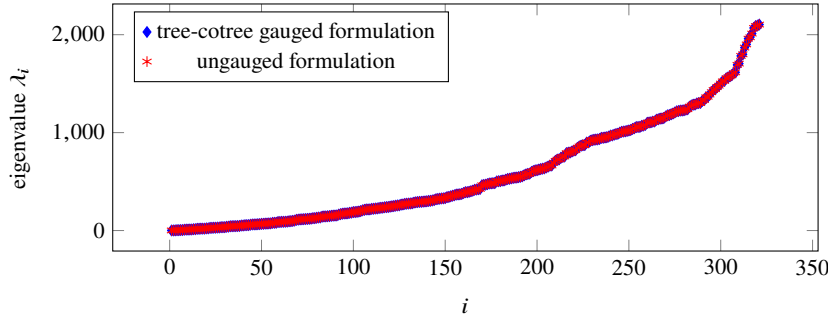


Fig. 8: Eigenvalues of the Maxwell eigenvalue problem of Example 2 for  $p = 1$  computed applying tree-cotree gauging and non-zero eigenvalues of the ungauged formulation.

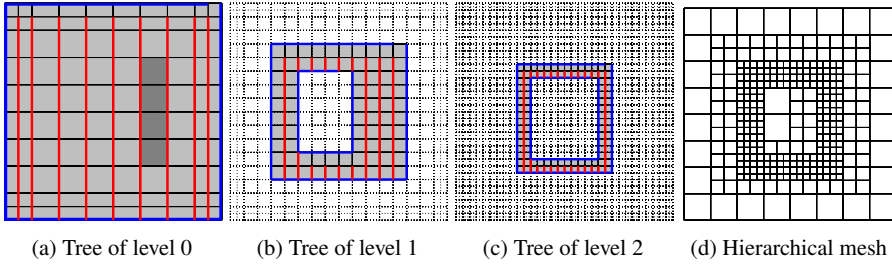


Fig. 9: Illustration of the trees built on each level for degree  $p = 3$ , for Example 2. The first three figures (a)-(c) show the tree of each single level, where the whole gray region corresponds to  $G_{\ell,\ell}$ , and the dark gray region corresponds to  $G_{\ell,\ell+1}$ . The blue edges correspond to the edges on the boundary of  $G_{\ell,\ell}$ , the red edges to the active edges, and the cyan edges to the deactivated edges. The right figure (d) shows the hierarchical mesh.

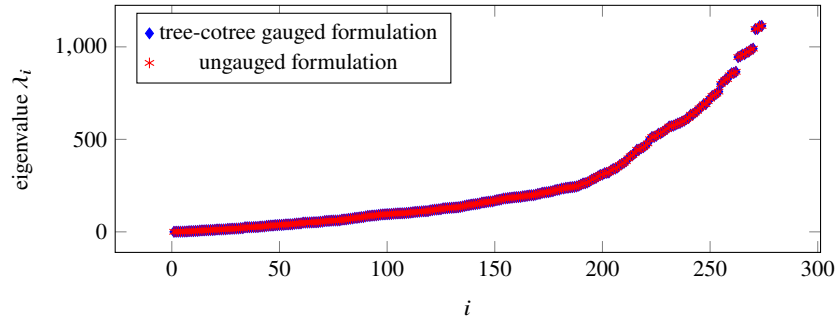


Fig. 10: Eigenvalues of the Maxwell eigenvalue problem of Example 2 for  $p = 3$  computed applying tree-cotree gauging and non-zero eigenvalues of the ungauged formulation.

1450/23-04 via the Hessian Ministry of Science and Art and the Hessen-Agentur and by the Association of Friends of TU Darmstadt via an Ernst Ludwig Mobility Grant.

## References

1. Albanese, R., Rubinacci, G.: Integral formulation for 3D eddy-current computation using edge elements. *IEE Proc. Sci. Meas. Tech.* **135**(7), 457–462 (1988). DOI 10.1049/ip-a-1:19880072
2. Alonso Rodríguez, A., Camaño, J., De Los Santos, E., Rapetti, F.: Weights for moments’ geometrical localization: a canonical isomorphism. *Adv. Comput. Math.* **50**(4) (2024). DOI 10.1007/s10444-024-10183-y
3. Bossavit, A.: *Computational Electromagnetism: Variational Formulations, Complementarity, Edge Elements*. Academic Press, San Diego, CA, USA (1998). DOI 10.1016/B978-0-12-118710-1.X5000-4
4. Buffa, A., Rivas, J., Sangalli, G., Vázquez Hernández, R.: Isogeometric discrete differential forms in three dimensions. *SIAM J. Numer. Anal.* **49**(2), 818–844 (2011). DOI 10.1137/100786708
5. Buffa, A., Sangalli, G., Vázquez, R.: Isogeometric analysis in electromagnetics: B-splines approximation. *Comput. Meth. Appl. Mech. Eng.* **199**, 1143–1152 (2010). DOI 10.1016/j.cma.2009.12.002
6. Buffa, A., Sangalli, G., Vázquez, R.: Isogeometric methods for computational electromagnetics: B-spline and t-spline discretizations. *J. Comput. Phys.* **257**, 1291–1320 (2013). DOI 10.1016/j.jcp.2013.08.015
7. Cabanas, D.C., Shepherd, K.M., Toshniwal, D., Vázquez, R.: Construction of exact refinements for the two-dimensional hierarchical B-spline de Rham complex (2025)
8. Evans, J.A., Scott, M.A., Shepherd, K.M., Thomas, D.C., Vázquez Hernández, R.: Hierarchical B-spline complexes of discrete differential forms. *IMA J. Numer. Anal.* **40**(1), 422–473 (2020)
9. Giannelli, C., Jüttler, B., Speleers, H.: THB-splines: The truncated basis for hierarchical splines. *CAGD* **29**(7, SI), 485–498 (2012). DOI 10.1016/j.cagd.2012.03.025
10. Hiptmair, R.: Multilevel gauging for edge elements. *Computing* **64**(2), 97–122 (2000). DOI 10.1007/s006070050005
11. Hughes, T.J.R., Cottrell, J.A., Bazilevs, Y.: Isogeometric analysis: CAD, finite elements, NURBS, exact geometry and mesh refinement. *Comput. Meth. Appl. Mech. Eng.* **194**, 4135–4195 (2005). DOI 10.1016/j.cma.2004.10.008



12. Jackson, J.D.: Classical Electrodynamics, 3rd edn. Wiley & Sons, New York, NY, USA (1998). DOI 10.1017/CBO9780511760396
13. Kapidani, B., Merkel, M., Schöps, S., Vázquez, R.: Tree-cotree decomposition of isogeometric mortared spaces in  $H(\text{curl})$  on multi-patch domains. *Comput. Meth. Appl. Mech. Eng.* **395**, 114949 (2022). DOI 10.1016/j.cma.2022.114949. Arxiv:2110.15860
14. Kapidani, B., Merkel, M., Schöps, S., Vázquez, R.: Arbitrary order spline representation of cohomology generators for isogeometric analysis of eddy current problems. *Adv. Comput. Math.* **50**(92) (2024). DOI 10.1007/s10444-024-10181-0. Arxiv:2310.14313
15. Kraft, R.: Adaptive and linearly independent multilevel  $B$ -splines. In: Surface fitting and multiresolution methods (Chamonix–Mont-Blanc, 1996), pp. 209–218. Vanderbilt Univ. Press, Nashville, TN (1997)
16. Kruskal, J.B.: On the shortest spanning subtree of a graph and the traveling salesman problem. *PROC* **7**(1), 48–50 (1956). DOI 10.2307/2033241
17. Mally, M., Kapidani, B., Merkel, M., Schöps, S., Vázquez, R.: Tree-cotree-based tearing and interconnecting for 3D magnetostatics: A dual-primal approach. *Comput. Meth. Appl. Mech. Eng.* **437**, 117737 (2025). DOI 10.1016/j.cma.2025.117737. Arxiv:2407.21707
18. Manges, J.B., Cendes, Z.J.: A generalized tree-cotree gauge for magnetic field computation. *IEEE Trans. Magn.* **31**(3), 1342–1347 (1995). DOI 10.1109/20.376275
19. Munteanu, I.: Tree-cotree condensation properties. *ICS Newslett.* **9**, 10–14 (2002). URL <https://www.compumag.org/wp/newsletter/>
20. Rapetti, F., Alonso Rodríguez, A., De Los Santos, E.: On the tree gauge in magnetostatics. *J* **5**(1), 52–63 (2022)
21. Ratnani, A., Sonnendrücker, E.: An arbitrary high-order spline finite element solver for the time domain Maxwell equations. *J. Sci. Comput.* **51**, 87–106 (2012)
22. Schöberl, J., Zaglmayr, S.: High order *nédélec* elements with local complete sequence properties. *COMPEL* **24**(2), 374–384 (2005). DOI 10.1108/03321640510586015
23. Shepherd, K., Toshniwal, D.: Locally-verifiable sufficient conditions for exactness of the hierarchical b-spline discrete de Rham complex in  $\mathbb{R}^n$ . *Found. Comput. Math.* (2024). DOI 10.1007/s10208-024-09659-6
24. Vuong, A.V., Giannelli, C., Jüttler, B., Simeon, B.: A hierarchical approach to adaptive local refinement in isogeometric analysis. *Comput. Meth. Appl. Mech. Eng.* **200**(49–52), 3554–3567 (2011). DOI 10.1016/j.cma.2011.09.004
25. Vázquez, R.: A new design for the implementation of isogeometric analysis in Octave and Matlab: GeoPDEs 3.0. *Comput. Math. Appl.* **72**(3), 523–554 (2016). DOI 10.1016/j.camwa.2016.05.010